HHS Public Access

Author manuscript

Cancer Cell. Author manuscript; available in PMC 2015 May 26.

Published in final edited form as:

Cancer Cell. 2014 April 14; 25(4): 455–468. doi:10.1016/j.ccr.2014.02.007.

SPOP promotes tumorigenesis by acting as a key regulatory hub in kidney cancer

Guoqiang Li[1,3,*], **Weimin Ci**[2,*], **Subhradip Karmakar**[4,5,*], **Ke Chen**[1], **Ruby Dhar**[4,5], **Zhixiang Fan**[9], **Zhongqiang Guo**[1,10], **Jing Zhang**[1], **Yuwen Ke**[1], **Lu Wang**[1,3], **Min Zhuang**[11], **Shengdi Hu**[12], **Xuesong Li**[10], **Liqun Zhou**[10], **Xianghong Li**[11], **Matthew F. Calabrese**[14], **Edmond R. Watson**[14], **Sandip M. Prasad**[7], **Carrie Rinker-Schaeffer**[7], **Scott E. Eggener**[7], **Thomas Stricker**[4,8], **Yong Tian**[13], **Brenda A. Schulman**[14,15], **Jiang Liu**[1,†], and **Kevin P. White**[4,5,6,†]

[1]CAS Key Laboratory of Genome Sciences and Information, Being Institute of Genomics, CAS, Beijing, 100101, China

[2]Laboratory of Disease Genomics and Individualized Medicine, Being Institute of Genomics, CAS, Beijing, 100101, China

[3]University of Chinese Academy of Sciences, Beijing, 100049, China

[4]Institute for Genomics and Systems Biology, University of Chicago and Argonne National Laboratory, Chicago, IL, 60637, USA

[5]Department of Human Genetics, University of Chicago, Chicago, IL, 60637, USA

[6]Department of Medicine, Section on Genetic Medicine, University of Chicago, Chicago, IL, 60637, USA

[7]Department of Surgery, Section of Urology, University of Chicago, Chicago, IL, 60637, USA

[8]Department of Pathology, University of Chicago, Chicago, IL, 60637, USA

[9]Kunming Medical University, Kunming, Yunnan, 650500, China

[10]Department of Urology, First Hospital of Peking University, Beijing, 100034, China

[11]Department of pathology, Peking University Cancer Hospital, Beijing, 100142, China

[12]Department of Pharmaceutical Chemistry, University of California San Francisco, San Francisco, CA, 94158, USA

[†]Correspondence: kpwhite@uchicago.edu (K.P.W.), liuj@big.ac.cn (J.L.).
[*]These authors contribute equally.

ACCESSION NUMBERS

The GEO accession number for the ChIP-seq data is GSE54327. The coordinates and structural data of the PTEN SBC motif binding with SPOP have been deposited to RCSB with accession number 4O1V.

SUPPLEMENTAL INFORMATION

Supplemental Information includes Supplemental Procedures, six figures, and one table.

[13]Laboratory of Animal Research Center, Institute of Biophysics, Chinese Academy of Sciences, Beijing, 100101, China

[14]Department of Structural Biology, St. Jude Children's Research Hospital, Memphis, TN, 38105, USA

[15]Howard Hughes Medical Institute, St. Jude Children's Research Hospital, Memphis, TN, 38105, USA

SUMMARY

Hypoxic stress and hypoxia-inducible factors (HIFs) play important roles in a wide range of tumors. We demonstrate that SPOP, which encodes an E3 ubiquitin ligase component, is a direct transcriptional target of HIFs in clear cell renal cell carcinoma (ccRCC). Furthermore, hypoxia results in cytoplasmic accumulation of SPOP which is sufficient to induce tumorigenesis. This tumorigenic activity occurs through the ubiquitination and degradation of multiple regulators of cellular proliferation and apoptosis, including the tumor suppressor PTEN, ERK phosphatases, the pro-apoptotic molecule Daxx and the Hedgehog pathway transcription factor Gli2. Knockdown of SPOP specifically kills ccRCC cells, indicating that it may be a promising therapeutic target. Collectively, our results indicate that SPOP serves as a regulatory hub to promote ccRCC tumorigenesis.

Graphical Abstract

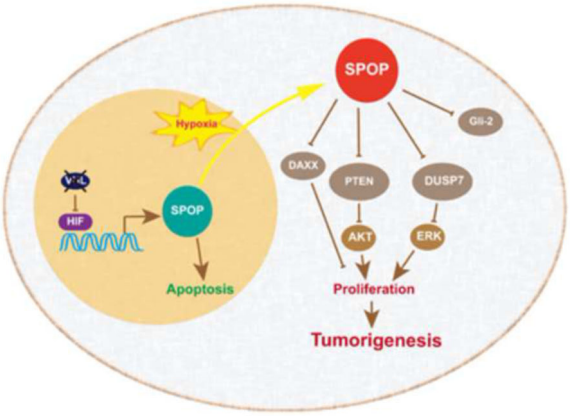

INTRODUCTION

Renal cell carcinoma (RCC) is the eighth leading malignancy in the United States, accounting for 4% of all cancers. More than 209,000 new cases and 102,000 deaths are estimated to occur worldwide each year (Rini et al., 2009). Approximately 30% of RCC patients present with metastatic disease at the time of diagnosis, and nearly half of the remainder will subsequently develop metastasis (McDermott et al., 2005; Negrier et al., 1998). As RCC is highly resistant to chemotherapy, first-line treatment of metastatic disease in the 1990s and 2000s relied on immunotherapies, such as Interleukin-2 and interferon alpha, despite low response rates (5 to 20%) (Fyfe et al., 1996; McDermott et al., 2005; Wardle, 1991). Hypoxic response mediated though HIFs is a key feature of most solid

tumors, but is particularly important in kidney cancers (Chi et al., 2006). Accordingly, recent targeted therapies that inhibit HIF-regulated pathways, including angiogenesis inhibitors directed against VEGF and PDGF signaling pathways have been developed. Although these therapies represent improvements in patient care, the majority of patients with advanced disease remain refractory to treatment, suggesting that certain critical HIF targets remain unknown (Escudier et al., 2007; Motzer et al., 2013; Motzer et al., 2007).

It has been shown that under normoxic conditions the oxygen-sensitive HIFα subunit is degraded by ubiquitination via the von Hippel-Lindau (VHL) tumor-suppressor gene (Kaelin, 2002). However, under hypoxic conditions HIF degradation is suppressed, leading to enhanced nuclear localization of HIF and transcription of various target genes, including the angiogenic gene VEGF (Kaelin Jr, 2008). Inactivating mutations or silencing of the VHL tumor suppressor gene can also suppress the degradation to HIF, and VHL mutation or silencing is found in at least 80% of all ccRCCs (Kim and Kaelin, 2004; Motzer and Molina, 2009; Nickerson et al., 2008). ccRCCs are the most common form of kidney cancer, accounting for 75% of all cases (Lopez-Beltran et al., 2006). Results from ccRCC xenograft experiments indicate that HIF accumulation is critical for VHL tumor suppressor function during ccRCC oncogenesis (Kaelin, 2008). It has also been found that renal carcinoma cells have evolved an alternative hypoxia signaling pathways compared with normal renal cells (Jiang et al., 2003) and the ccRCCs are in a high hypoxia response state compared to the normal kidney samples and other subtypes of kidney cancer (Chi et al., 2006).

Although hypoxia response plays a critical role in kidney cancer, other cell regulatory pathways are also important for tumor development and progression (Brugarolas, 2007). For example, another promising target for RCC therapies is the mammalian Target of Rapamycin (mTOR) pathway, which is abnormally activated during the development of kidney cancer (Robb et al., 2007). mTOR is negatively regulated by the tumor suppressor PTEN (Hollander et al., 2011), which is mutated or down-regulated in many cancers, including ccRCC (Vivanco and Sawyers, 2002). The mTOR pathway positively regulates cell growth and proliferation through enhanced mRNA translation by phosphorylated S6 kinase1 (S6K1) and 4E binding protein-1 (4E-BP1) (Sarbassov et al., 2005). In spite of its promise, the mTOR inhibitor temsirolimus produces only low objective responses in patients with advanced RCC, although it contributes to a modest improvement in overall survival (Hudes et al., 2007; Kapoor and Figlin, 2009). Further investigation of the mechanisms of PTEN down-regulation in ccRCC is critical for an understanding of RCC pathogenesis.

Our previous studies demonstrated that the SPOP protein is overexpressed in 85% of kidney cancers and that nearly 100% of primary and metastatic ccRCCs exhibit SPOP accumulation (Liu et al., 2009). SPOP is a BTB/POZ domain protein, and MEL-26, the *C. elegans* SPOP ortholog, was first identified as an adaptor for the E3 ligase Cullin3 (Cul3). In *C. elegans*, MEL-26 promotes the meiotic/mitotic transition through the degradation of MEI-1/katanin (Mains et al., 1990; Pintard et al., 2003; Xu et al., 2003). In *Drosophila*, D-SPOP (also known as Roadkill) can promote the ubiquitination and degradation of the Gli transcription factor ortholog Cubitus interruptus (Ci) and the JNK phosphatase Puckered to regulate the Hedgehog (Hh) and Tumor Necrosis Factor (TNF) pathways, respectively (Kent et al., 2006;

Zhang et al., 2006)(Liu et al., 2009). In humans, the roles for SPOP in regulating the Hh and TNF pathways have been conserved (Zhang et al., 2006) (Liu et al., 2009), and several other SPOP substrates have been identified as well, including the death domain–associated protein (Daxx) (Kwon et al., 2006), the polycomb group protein BMI-1, and the Histone variant MacroH2A (Hernandez-Munoz et al., 2005). Together these previous results indicate that SPOP plays important roles during cell apoptosis, proliferation and animal development, and suggest that overexpression of SPOP in ccRCCs may lead to dysregulation of pathways involved in tumorigenesis. However, it is unclear how SPOP becomes overexpressed or whether it may function directly in kidney tumorigenesis. Adding to this puzzle, recent deep sequencing studies of breast, prostate and endometrial cancers found that SPOP is frequently mutated, and the SPOP locus is observed to undergo loss of heterozygosity (LOH), indicating that SPOP may act as a tumor suppressor (Berger et al., 2011; Li et al., 2011). However, no SPOP mutations have been detected in kidney cancers thus far (Liu et al., 2009; The Cancer Genome Atlas Research, 2013). In this study, we aim to determine whether SPOP promotes tumorigenesis in kidney.

RESULTS

HIF regulates SPOP expression

Immunohistochemistry results have suggested that SPOP is overexpressed in virtually all ccRCCs (Liu et al., 2009). We confirmed this finding by immunoblot assays in multiple pairs of ccRCC primary tumor tissue and matched normal adjacent tissue (Figure 1A). However, the mechanism underlying this SPOP overexpression is unknown. Considering the frequent accumulation of HIF in ccRCC patients, we were interested whether HIF can drive SPOP overexpression. We identified a HIF-1α binding peak in the first intron of SPOP by ChIP-seq (Figure 1B) and further validated it by ChIP-qPCR (Figure S1A). To determine whether this intronic DNA sequence region functions as a HIF-responsive regulatory element, we performed a luciferase reporter assay by inserting the wild-type HIF binding sequence into a pGL3-promoter reporter vector. In human embryonic kidney HEK293 cells, the wild-type sequence exhibits increased luciferase activity under hypoxic exposure (1% O_2/5% CO_2/94% N_2) compared to normoxia, while HIF-1α knockdown impairs the luciferase activity (Figure 1C). Additionally, we constructed several mutations or deletions of the predicted hypoxia-response elements (HRE; 5'-RCGTG-3' and 5'-[A/C]ACAG-3') (Miyazaki et al., 2002). Although mutants of CACAG showed marginal decrease in luciferase activity (Figure S1B), both point mutations and deletion of CGTG site showed significant decrease in luciferase activity (Figure 1C), demonstrating that the HIF binding site is functional in this hypoxia-responsivecis-regulatory element.

To further elucidate whether HIF can regulate SPOP, the VHL wild-type ccRCC cell line Caki-2 was cultured under hypoxic conditions. Hypoxic culture resulted in the accumulation of HIF-1α and HIF-2α proteins. Both SPOP mRNA (Figure 1D) and protein (Figure 1E) levels increased in ccRCC cells under hypoxic conditions. Additionally, ectopic overexpression of either HIF-1α or HIF-2α led to SPOP accumulation in HEK293 cells (Figure 1F), indicating that both HIF-1α and HIF-2α can regulate SPOP expression. Although knockdown of HIF-1α alone in Caki-2 cells which express both HIF-1α and

HIF-2α (Kucejova et al., 2011) can reduce SPOP protein abundance (Figure 1G), double-knockdown of HIF-1α and HIF-2α is more effective than either alone (Figure S1C). Consistent with these results, knocking down HIF-2α by siRNA in the ccRCC cell line A498 that predominantly expresses HIF-2α (Shinojima et al., 2007) resulted in a reduction in the mRNA (Figure 1H) and protein (Figure 1I) abundance of SPOP, as well as the known HIF target VEGF. Because VHL mutation is one of the most common causes of kidney cancer and affects abundance of HIFs, we examined SPOP abundance after restoring VHL in the VHL-null cell lines 786-O and A498. Accordingly, restoration of VHL led to decreased protein abundance of SPOP (Figure 1J), and conversely VHL-knockdown in HEK293 cells resulted in an increase in SPOP (Figure S1D). Taken together, these results demonstrate that HIF can directly regulate SPOP expression.

SPOP accumulation in the cytoplasm of ccRCC cells

SPOP was first identified as a nuclear protein (Nagai et al., 1997), and several studies have confirmed its nuclear location in HEK293 and HeLa cells (Bunce et al., 2008; Hernandez-Munoz et al., 2005; Kwon et al., 2006). To investigate SPOP localization in kidney cancer, we used a monoclonal anti-SPOP antibody (Liu et al., 2009) to stain kidney tissue biopsies. We found that SPOP was predominately localized in the nucleus of normal kidney tissue. However, we observed SPOP accumulation in the cytoplasm of neoplastic ccRCC cells, with residual SPOP remaining in the nucleus (Figure 2A). Immunocytochemistry staining also revealed that SPOP predominately accumulated in the cytoplasm of Caki-2 cells but was primarily localized within the nucleus of HeLa (Figure 2B) and HEK293 cells (Figure S2A). Ectopically expressed GFP-tagged SPOP in ccRCC cell lines (Caki-2 and A498) and in non-ccRCC cell lines (HEK293 and HeLa cells) yielded similar results as endogenous SPOP (Figure S2B). Furthermore, cell fractionation assays confirmed the cytoplasmic localization of SPOP in ccRCC cell lines and predominantly nuclear localization in HEK293 cells (Figure S2C).

Hypoxia drives SPOP accumulation in the cytoplasm

Previous studies have shown that some proteins accumulate in the cytoplasm under stress conditions, such as hypoxia, heat shock and arsenite exposure (Arimoto et al., 2008). Given that ccRCC tumorigenesis is associated with hypoxia signaling, we tested whether hypoxic conditions could stimulate SPOP accumulation in the cytoplasm. Immunofluorescence staining showed that endogenous SPOP localizes in the nucleus of HeLa cells under normoxia, while hypoxic treatment (1% O_2/5% CO_2/94% N_2) led to SPOP accumulation in the cytoplasm (Figure 2B). Additionally, HIF overexpression further enhanced the cytoplasmic accumulation of SPOP (Figure 2B). SPOP accumulation in the cytoplasm under hypoxic treatment was further confirmed by cell fractionation assays (Figures 2C and 2D). Although previous data showed that ectopically expressed GFP-SPOP localized in the nucleus of HeLa and HEK293 cells under normoxia (Figure S2B), we found that it also accumulated in the cytoplasm under hypoxia in these cells (Figure S2D). Thus, hypoxia appears to be a sufficient condition to stimulate the cytoplasmic accumulation of SPOP.

Cytoplasmic SPOP promotes tumorigenesis

Next, we wished to test whether cytoplasmic SPOP is associated with tumorigenic phenotypes. Sequence analysis indicated that SPOP contains a nuclear localization signal (NLS) at its C-terminus, amino acids 367–373 (PRKRLKQ). Crystallographic analysis indicates that the deletion of the NLS peptide from the SPOP C-terminus is unlikely to affect the binding of SPOP with the E3 ligase Cullin3 or SPOP substrates (Zhuang et al., 2009). Additionally, the *in vitro* ubiquitination of SPOP substrates is unaffected by deletion of the NLS from SPOP (Zhuang et al., 2009). Therefore, we deleted the NLS peptide from SPOP to test whether SPOP lacking the NLS would accumulate in the cytoplasm when ectopically expressed in non-ccRCC cells. As expected, ectopic expression of GFP-SPOP lacking the NLS accumulates in the cytoplasm of HEK293 cells (Figure S2E). We refer to SPOP lacking the NLS as SPOP-cyto.

We overexpressed SPOP-cyto and wild type SPOP in non-ccRCC cell lines to determine whether there are differences in phenotypic effects. A BrdU incorporation assay showed that wild type SPOP inhibited cell proliferation (Figure 3A), consistent with previous results that SPOP can induce apoptosis in HEK293 (Liu et al., 2009) and HeLa cells (Kwon et al., 2006) (Figure S3A). Strikingly, SPOP-cyto enhanced proliferation rather than inducing apoptosis (Figure 3A). As a marker for apoptotic state of the cells, we used the pro-apoptotic protein Bax that has been shown to be inactivated by phosphorylation at Ser184 (Gardai et al., 2004). Overexpression of SPOP-cyto increased the level of Ser184-phosphorylated Bax (p-Bax), indicating that SPOP-cyto can inhibit Bax-mediated apoptosis (Figure 3B). Overexpression of SPOP-cyto also increased the protein abundance of the cellular proliferation markers phospho-histone H3 (p-Histone H3)(Bhatia et al., 2011) and Proliferating Cell Nuclear Antigen (PCNA), consistent with the observation that SPOP-cyto promotes cell proliferation (Figure 3B). Thus, the accumulation of cytoplasmic SPOP appears to alter the function of the protein in comparison to its nuclear form, changing SPOP function from pro-apoptotic to anti-apoptotic and pro-proliferative. Furthermore, siRNA-knockdown of SPOP (Figure S3B) induced apoptosis in ccRCC cells where SPOP is in the cytoplasm, but not in HeLa or HEK293 cells (Figure 3C, S3C and S3D). Knockdown of SPOP in ccRCC cells also resulted in decreased levels of p-Bax (Ser184), PCNA, and p-Histone H3 levels (Figure S3E). However, we wondered whether hypoxia-induced cytoplasmic localization of SPOP in non-ccRCC cells would also lead to an SPOP "addicted" state where knockdown of SPOP would lead to cell death. Indeed, RNAi knockdown of SPOP in HeLa cells under hypoxia exposure led to significantly increased apoptosis compared to cells treated with only hypoxia stress (Figure S3F), similar to results of SPOP knock-down in ccRCC cell lines. Together these results indicate that inhibition of SPOP can specifically induce apoptosis and inhibit proliferation in ccRCC cells but not in non-ccRCC cells, suggesting that SPOP may serve as a therapeutic target specific to cancer cells.

We further investigated whether cytoplasmic SPOP could promote tumorigenesis in a nude mouse xenograft model. HEK293 cells have previously been used to demonstrate the tumorigenic potential of oncogenes (Hamid et al., 2005). We generated stable polyclonal HEK293 cell lines transfected with SPOP-cyto, SPOP or empty vector (pcDNA3) (Figure

S3G), and the levels of exogenous SPOP-cyto and SPOP are comparable to the endogenous protein in primary ccRCC samples (Figure 1A). Subcutaneous injection of the stably transfected HEK293-SPOP-cyto cells into nude mice induced tumor formation in approximately 80% of mice (15/19) within 6 weeks, whereas wild type SPOP and control empty vector produced no visible tumor growth (0/19 and 0/19, respectively) (Figure 3D). Further, histopathologic analyses of the xenograft tumors reveal typical cancerous lesions (Figure S3H). Thus, cytoplasmic SPOP, but not nuclear SPOP, promotes tumorigenesis.

SPOP mediates the ubiquitination and degradation of tumor suppressor PTEN

We next wished to investigate the mechanism by which cytoplasmic SPOP promotes tumorigenesis. SPOP was previously identified as a regulatory 'hub' molecule in *Drosophila* (Liu et al., 2009) and can degrade substrates in multiple signaling pathways via Cul3-mediated ubiquitination (Bunce et al., 2008; Hernandez-Munoz et al., 2005; Kwon et al., 2006; Xu et al., 2003; Zhuang et al., 2009). SPOP crystal structure studies demonstrated that all known SPOP substrates share a conserved SPOP-binding consensus (SBC) motif (Φ-π-S-S/T-S/T; Φ is nonpolar, π is polar) (Zhuang et al., 2009). Thus, we hypothesized that cytoplasmic SPOP might promote cancer phenotypes by mediating the degradation of cytoplasmic proteins that contain SBC motifs.

Previously, we found that SPOP can mediate the ubiquitination and degradation of Puc, a Dual-Specificity Phosphatase (DUSP) class molecule in *Drosophila* that regulates JNK signaling (Liu et al., 2009). DUSPs have been implicated as major modulators of critical signaling pathways that are dysregulated in various diseases (Patterson et al., 2009). Therefore, we computationally searched the human proteome for DUSP domain proteins that contain the SBC motif. We found seven DUSP domain containing proteins with at least one SBC motif (Table S1), including the cytoplasmic tumor suppressor protein PTEN with substrate specificity to phosphatidylinositol phosphates (Myers et al., 1998) and which contains the SBC motif ASSST (residues 359–363).

Genetic alterations targeting the PTEN tumor suppressor are among the most frequently noted somatic mutations in human cancers (Sansal and Sellers, 2004). PTEN functions to antagonize phosphoinositide 3-kinase (PI3K)/Akt signaling through its lipid phosphatase activity, thereby controlling cell growth, survival, and metabolic processes (Wu et al., 1998). Based on previous crystal structures, the SBC motif in PTEN is in a flexible region that is not folded into any three-dimensional domains and is thus potentially accessible for SPOP binding (Lee et al., 1999). To understand the molecular basis for potential SPOP MATH domain interactions with the PTEN SBC, we determined the crystal structure of the SPOP MATH complex with a peptide corresponding to PTEN residues 354–368, which comprises the PTEN SBC motif. The SPOP MATH domain forms an anti-parallel β-sandwich, and the PTEN SBC motif adopts an extended conformation to bind within the MATH central shallow groove (Figure S4A and S4B). SPOP MATH-SBC interactions are anchored by both hydrophobic and polar interactions with the PTEN SBC residues ASSST (Figure 4A).

We further validated whether PTEN acts as a SPOP substrate in cells. Co-immunoprecipitation (Co-IP) data showed that both SPOP and SPOP-cyto can bind PTEN, whereas the deletion of the PTEN SBC motif eliminated binding (Figure 4B).

Overexpressed SPOP-cyto also bound endogenous PTEN in HeLa cells (Figure 4C). Furthermore, exogenous PTEN abundance was reduced when PTEN was co-expressed with SPOP-cyto in HeLa cells, whereas a PTEN SBC mutant was resistant to SPOP-cyto-mediated degradation (Figure 4D). A cycloheximide (CHX) chase assay also indicated that PTEN is rapidly degraded by SPOP-cyto after co-transfection (Figure 4E). Importantly, SPOP can mediate the ubiquitination of PTEN but the SBC mutated PTEN was not affected by SPOP, as demonstrated by *in vivo* (Figure 4F) and *in vitro* ubiquitination assays (Figure 4G, Figure S4C). Taken together, these results indicate that SPOP promotes the degradation of tumor suppressor PTEN.

SPOP mediates the degradation of ERK phosphatase DUSP7

Our computational scan for SBC motifs also indicated that DUSP6 and DUSP7, ERK-specific cytoplasmic MAPK phosphatases, are candidate SPOP targets (Table S1). DUSP6 contains the motif CSSSS (residues 155–159), and DUSP7 contains the motif VDSSS (residues 191–195). The classical ERK pathway has long been associated with the ability of cancer cells to grow independently, and this pathway is dysregulated in approximately 30% of human tumors (Dhillon et al., 2007; Keyse, 2008). Reports from several groups have indicated that the level of ERK phosphorylation is significantly elevated in ccRCC (Campbell et al., 2009; Lee et al., 2009). We found that the levels of ERK phosphorylation increased after dual knockdown of DUSP6 and DUSP7 in Caki-2 cells (Figure S5A), indicating that DUSP6 and DUSP7 regulate the ERK pathway in ccRCC cells.

Based on their SBC domains DUSP6 and DUSP7 have similar predicted SPOP interaction properties, we focused our biochemical analysis on DUSP7. Co-IP assays showed that both SPOP and SPOP-cyto bind DUSP7, whereas a mutant DUSP7 SBC motif eliminated binding with SPOP (Figure 5A). Furthermore, overexpressed SPOP-cyto bound to endogenous DUSP7 in HeLa cells (Figure 5B). DUSP7 is also down-regulated in SPOP and SPOP-cyto overexpressing cells (Figure 5C), while neither SPOP nor SPOP-cyto can degrade the DUSP7-SBC mutant (Figure 5D). A cycloheximide (CHX) chase assay indicated that DUSP7 is rapidly degraded by SPOP-cyto (Figure S5B). Importantly, SPOP mediated the ubiquitination of DUSP7 but not its SBC mutant in both *in vivo* (Figure 5E) and *in vitro* ubiquitination assays (Figure 5F, Figure S5C).

Cytoplasmic SPOP acts as a regulatory hub by modulating multiple pathways during kidney tumorigenesis

PI3K/Akt and ERK pathways are hyper-activated in different types of tumors including ccRCC (Campbell et al., 2009; Lee et al., 2009). While it has been shown that these pathways are sometimes genetically altered in ccRCC, such mutations contribute to a limited percentage of ccRCC patients (Network, 2013; Sato et al., 2013). Considering that SPOP is overexpressed in nearly 100% of ccRCCs, we wondered whether cytoplasmic SPOP might deregulate these pathways through mediating degradation of PTEN, DUSP6 and DUSP7 in ccRCC. Thus, we examined the effects of RNAi knockdown of SPOP on these signaling pathways in A498 ccRCC cells. As shown in Figure 6A, SPOP knockdown resulted in increased levels of PTEN and DUSP7, and a decrease in phosphorylated Akt levels and

ERK, respectively (Figure 6A). These results indicate that SPOP can deregulate these pathways by degrading PTEN and DUSP7 in ccRCC.

SPOP has been found to also degrade many other substrates, some of which are candidates for promoting tumorigenesis if post-translationally degraded, including Daxx (Kwon et al., 2006) and Gli2 (Wang et al.). Daxx protein is expressed in both the nucleus and cytoplasm. In the cytoplasm, Daxx has been reported to interact with ASK1 and other apical kinases to induce cell death (Salomoni and Khelifi, 2006). Degradation of Daxx would impair the ability of the cells to respond to apoptotic cues. Gli2 acts as a mediator of Hh signaling, and has both transcriptional repression and activation domains (Sasaki et al., 1999). Gli2 is primarily localized in cytoplasm and can transfer to nucleus under Hh stimulation (Kim et al., 2009). Both Daxx and Gli2 are upregulated when SPOP is knocked down in Caki-2 ccRCC cells (Figure 6B). Additionally, knockdown of Gli2 in ccRCC cells showed a further increase in the proliferation marker p-Histone H3 (Figure S6A). To further explore the possibility that cytoplasmic SPOP degrades these key substrates in ccRCC, we examined their protein abundance under hypoxic exposure in non-ccRCC cells. As expected, the abundance of PTEN, DUSP7 and Daxx proteins were all reduced in HeLa cells when SPOP was increased and accumulated in the cytoplasm under hypoxia (Figure 6C).

To further validate the role of SPOP on these targets, we examined the abundance of these SPOP targets in primary ccRCC tissue samples. We found an inverse relationship between PTEN levels and SPOP levels in 100% (14/14) of examined primary ccRCC tumor samples. These ccRCC tumor tissues exhibited high levels of SPOP and low levels of PTEN, consistent with previous reports that PTEN levels are reduced in ccRCCs (Brenner et al., 2002). By contrast, normal adjacent kidney tissues exhibit the opposite relationship (Figure 6D). Similarly, we observed inverse relationships for all other examined substrates, DUSP7 (10/10), Daxx (14/14) and Gli2 (14/14).

Finally, to determine whether the decrease of SPOP targets promotes ccRCC tumor cell survival, we restored PTEN and DUSP7 by ectopically expression in A498 ccRCC cells and found that cellular apoptosis was strongly induced (Figure 6E). Consistent with this finding, knockdown of DUSP6 and DUSP7 together led to an increase of cell proliferation in ccRCC cells (Figure S6B and S6C).

DISCUSSION

Our results indicate that HIF can drive SPOP over-expression in ccRCC and over-expressed SPOP accumulates in the cytoplasm of ccRCC. In turn, accumulation of cytoplasmic SPOP in ccRCC cells appears to directly result in the degradation of PTEN, DUSP6, DUSP7, Daxx, and Gli2. We suggest that the concerted loss of function of these proteins in ccRCCs leads to tumorigenic phenotypes. Therefore, cytoplasmic SPOP appears to drive tumorigenesis by acting as a key regulatory ‘hub’ protein that orchestrates cancer phenotypes through the modulation of several critical cellular pathways (Figure 6F).

The HIF signaling pathway and the PTEN/mTOR pathway are currently the major therapeutic targets in ccRCC treatment. We suggest here that, as a regulatory hub driving

tumorigenesis in ccRCC, SPOP has potential to be an efficient drug target. Knocking down SPOP leads to apoptosis in ccRCC cell lines but not in HEK293 and HeLa cells, where SPOP is in the nucleus. In addition to considering SPOP itself as a target, we also suggest that combinatorial modulation of the signaling pathways regulated by SPOP may have the potential to be more effective than the current targeted therapies alone.

Several issues about SPOP function in ccRCC remain to be explored. For example, given the promiscuity of SPOP in targeting critical proliferative and apoptotic pathway components, it is unlikely that the proteins studied here are the only critical cellular targets. While we focused our discovery of new targets on proteins with DUSP domains, genome-wide there are dozens of potential SPOP substrates. However, the modulation of PTEN, ERK, and Hh (through Gli2) signaling clearly has major effects on proliferation, and these results clearly demonstrate that SPOP is acting as a critical hub in a network involving multiple cancer-related pathways. In doing so, SPOP appears to be both necessary and sufficient for tumorigenic phenotypes.

Another open question is what molecular mechanism accounts for SPOP mislocalization to the cytoplasm. Although we demonstrate that hypoxia can drive accumulation of SPOP in cytoplasm, a number of possibilities exist for how it transfers from the nucleus to the cytoplasm or vice versa. Since no SPOP mutation has been detected in kidney cancers thus far (Liu et al., 2009; The Cancer Genome Atlas Research, 2013), post-transcriptional modifications on SPOP, such as phosphorylation and ubiquitination on its nuclear localization signal, may regulate its location. It has been extensively reviewed elsewhere that post-transcriptional modifications can regulate nuclear import (Hung and Link, 2011; Nardozzi et al., 2010). Alternatively, this translocation may also be regulated by interaction with transfer proteins regulated by hypoxia, since protein–protein interactions also serve as an important regulatory mechanism of protein translocation (Hung and Link, 2011). Localized and targeted degradation of SPOP is also an intriguing mechanism, although attempts in our hands to determine whether it could be a target of obvious candidates such as VHL have been negative (Karmakar et al., unpublished data). Exploring the molecular mechanisms of cytoplasmic SPOP accumulation is an important direction to pursue in the future.

Finally, our previous screening also observed that SPOP was overexpressed in several other tumors, including some cases of endometrial and germ cell tumors (Liu et al., 2009). The role of SPOP in these tumor types is unexplored, as is the role of mutant SPOP or its LOH in prostate and breast cancers (Berger et al., 2011; Li et al., 2011). The identification of loss-of-function SPOP in these other tissues warrants the caution in development of any therapeutic interventions that systemically inhibit SPOP function. Indeed, SPOP may be acting as a tumor suppressor in breast and/or prostate cancers, but our results clearly indicate that it acts as an oncoprotein in ccRCCs. Considering hypoxia stress plays important roles in many different tumors, future efforts to develop tools that selectively modulate SPOP may be beneficial for treating a wide range of tumors.

EXPERIMENTAL PROCEDURES

Chromatin immunoprecipitation (ChIP)

ChIP was performed as previously described (Polo et al., 2008). Briefly, ChIPs for HIF-1α were performed with 10 to 20 × 10^6 Caki-2 cells under normoxic and hypoxic conditions using 5 ug HIF-1α antibody (Novus, NB100-134). An IgG antibody (Upstate Biotechnology) was used as a negative control. Enriched DNA fragments were detected by qPCR and are presented as enrichment relative to input.

Luciferase reporter assay

DNA fragments spanning the potential HIF binding peak in SPOP (chr17:45,109,830-45,109,897 and a serial mutants to the potential hypoxia-response elements (HRE) were cloned into PGL4.23 [luc2/minP] vector (Promega, E841A). Plasmids were then co-transfected in K293 cells with a transfection controlling plasmid pGL4.23 [hRluc/TK] (Promega, E692A). After 24 hr, cells were transfected with two independent siRNA oligos to HIF-1α (Dharmacon, J-004018-07 and J-004018-10) and further cultured under normoxic and hypoxic (1% O_2/5% CO_2/94% N_2) condition for another 20 hours. Luciferase activity was measured using the Dual-glo luciferase kit (Promega, E2920).

Immunohistochemistry

Primary human kidney cancer samples were obtained from the Department of Urology, First Hospital of Peking University with patients' consent and approval of the institutional review board of Peking University. Immunohistochemistry was performed according to the method previously used (Cen et al., 2007) with appropriate antibodies (Supplemental Experimental Procedures).

Immunofluorescence microscopy

Immunofluorescence was carried out as described (Gottfried et al., 2004). Mouse anti-SPOP mAb (clone 5G) was used as the primary antibody. The slides were examined using a Leica Tcs Sp5 confocal laser scanning microscope (Supplemental Experimental Procedures).

Proliferation assay

HEK293 cells were transfected with SPOP, SPOP-cyto or control empty vector. Cell proliferation was measured by BrdU incorporation (Roche, Cell proliferation ELISA kit) according to the manufacturer's instructions.

Apoptosis assay

Caspase 3/7 activities were measured using the Apo-ONE® Homogenous Caspase Assay kit (Promega) according to the manufacturer's instructions. After incubated for 2 hr at room temperature, fluorescence was detected by a Fluoroskan Ascent FL microplate reader (Thermo Scientific).

Tumor xenograft experiments

Stable HEK293 cell lines expressing SPOP, SPOP-cyto or the control empty vector were established as previously described (Kass et al., 2007). Briefly, a total of 5×10^6 tumor cells were injected subcutaneously into BALB/c nude mice. Animals were sacrificed at 6 weeks after cell injection to investigate the tumor formation. A total of 19 mice were used for each construct with experiments replicated under similar conditions at the Chinese Academy of Science and The University of Chicago. All of the animal experiments were approved by the Committee on the Use of Live Animals in Teaching and Research at the Institute of Biophysics, CAS as well as the Institutional Care and Use Committee at the University of Chicago in accordance with the NIH Guide for the Care and Use of Laboratory Animals.

Immunoprecipitation

Cells were transiently transfected with the indicated plasmids. Twenty-four hours after transfection, cells were harvested with RIPA buffer and briefly sonicated at 4°C. Lysates were immunoprecipitated with anti-myc or anti-flag conjugated agarose beads (Sigma). Precipitates were analyzed on SDS–polyacrylamide gels.

In vivo ubiquitination assay

In vivo ubiquitination assays were based on the protocol previously described (Liu et al., 2009). Briefly, HeLa cells were transfected with the indicated plasmids. Twenty-four hours after transfection, cells were treated with 10 μM MG132 (Calbiochem) for 4 hr before harvesting. Cells were then lysed in denaturing buffer (1% SDS/50mM Tris [pH 7.5], 0.5mM EDTA/1mM DTT). After incubation for 5 min at 100°C, the lysate was sonicated and diluted 10 times with RIPA lysis buffer and subjected to co-immunoprecipitation with anti-c-myc-conjugated agarose beads (Sigma, rabbit antibody) followed by immunoblotting analysis with anti-HA antibody (Sigma, H9658).

In vitro ubiquitination assay

In vitro ubiquitination was performed as reported previously (Zhuang et al., 2009) (Supplemental Experimental Procedures).

Supplementary Material

Refer to Web version on PubMed Central for supplementary material.

ACKNOWLEDGEMENTS

We thank Erin E. Mowers for critical reading and editing of the manuscript. W.C. was supported by the 973 Program from MOST 2011CB510101. K.Y. was supported by National 863 High Tech Foundation SS2014AA020608. K.C was supported by NSFC 81101940. W.C. was supported by NSFC 91231112 and 31171244. E.E.M. was supported by the University of Chicago Naomi Ragins-Goldsmith endowed fellowship and the University of Chicago MSTP Training Grant T32 GM007281. M.C. was supported by an HHMI postdoctoral fellowship from the Damon Runyon Cancer Research Foundation DRG 2021-9. T.S. was supported by a National Research Service Award from the United States National Institutes of Health. B.S. was supported by ALSAC, HHMI, NIH 5R01GM069530, and NIH 5P30CA021765. Y.T. was supported by the CAS 09CF011001. J.L. was supported by grants from 973 Program MOST 2011CB510101, NSFC 81171902, and Beijing Science Foundation 5102031. K.P.W. was supported by the W.M. Keck Foundation, the United States National Institute of General Medical Sciences P50GM081892, and by the Searle Funds at The Chicago Community Trust from the Chicago Biomedical Consortium.

REFERENCES

Arimoto K, Fukuda H, Imajoh-Ohmi S, Saito H, Takekawa M. Formation of stress granules inhibits apoptosis by suppressing stress-responsive MAPK pathways. Nat Cell Biol. 2008; 10:1324–1332. [PubMed: 18836437]

Berger MF, Lawrence MS, Demichelis F, Drier Y, Cibulskis K, Sivachenko AY, Sboner A, Esgueva R, Pflueger D, Sougnez C, et al. The genomic complexity of primary human prostate cancer. Nature. 2011; 470:214–220. [PubMed: 21307934]

Bhatia B, Hsieh M, Kenney AM, Nahle Z. Mitogenic Sonic hedgehog signaling drives E2F1-dependent lipogenesis in progenitor cells and medulloblastoma. Oncogene. 2011; 30:410–422. [PubMed: 20890301]

Brenner W, Farber G, Herget T, Lehr HA, Hengstler JG, Thuroff JW. Loss of tumor suppressor protein PTEN during renal carcinogenesis. Int J Cancer. 2002; 99:53–57. [PubMed: 11948491]

Brugarolas J. Renal-Cell Carcinoma — Molecular Pathways and Therapies. New England Journal of Medicine. 2007; 356:185–187. [PubMed: 17215538]

Bunce MW, Boronenkov IV, Anderson RA. Coordinated activation of the nuclear ubiquitin ligase Cul3-SPOP by the generation of phosphatidylinositol 5-phosphate. J Biol Chem. 2008; 283:8678–8686. [PubMed: 18218622]

Campbell L, Nuttall R, Griffiths D, Gumbleton M. Activated extracellular signal-regulated kinase is an independent prognostic factor in clinically confined renal cell carcinoma. Cancer. 2009; 115:3457–3467. [PubMed: 19526593]

Cen L, Arnoczky KJ, Hsieh F-C, Lin H-J, Qualman SJ, Yu S, Xiang H, Lin J. Phosphorylation profiles of protein kinases in alveolar and embryonal rhabdomyosarcoma. Mod Pathol. 2007; 20:936–946. [PubMed: 17585318]

Chi J-T, Wang Z, Nuyten DSA, Rodriguez EH, Schaner ME, Salim A, Wang Y, Kristensen GB, Helland Å, Børresen-Dale A-L, et al. Gene Expression Programs in Response to Hypoxia: Cell Type Specificity and Prognostic Significance in Human Cancers. PLoS Med. 2006; 3:e47. [PubMed: 16417408]

Dhillon AS, Hagan S, Rath O, Kolch W. MAP kinase signalling pathways in cancer. Oncogene. 2007; 26:3279–3290. [PubMed: 17496922]

Escudier B, Eisen T, Stadler WM, Szczylik C, Oudard S, Siebels M, Negrier S, Chevreau C, Solska E, Desai AA, et al. Sorafenib in advanced clear-cell renal-cell carcinoma. N Engl J Med. 2007; 356:125–134. [PubMed: 17215530]

Fyfe GA, Fisher RI, Rosenberg SA, Sznol M, Parkinson DR, Louie AC. Long-term response data for 255 patients with metastatic renal cell carcinoma treated with high-dose recombinant interleukin-2 therapy. J Clin Oncol. 1996; 14:2410–2411. [PubMed: 8708739]

Gardai SJ, Whitlock BB, Xiao YQ, Bratton DB, Henson PM. Oxidants inhibit ERK/MAPK and prevent its ability to delay neutrophil apoptosis downstream of mitochondrial changes and at the level of XIAP. J Biol Chem. 2004; 279:44695–44703. [PubMed: 15292176]

Gottfried Y, Rotem A, Lotan R, Steller H, Larisch S. The mitochondrial ARTS protein promotes apoptosis through targeting XIAP. EMBO J. 2004; 23:1627–1635. [PubMed: 15029247]

Hamid T, Malik MT, Kakar SS. Ectopic expression of PTTG1/securin promotes tumorigenesis in human embryonic kidney cells. Mol Cancer. 2005; 4:3. [PubMed: 15649325]

Hernandez-Munoz I, Lund AH, van der Stoop P, Boutsma E, Muijrers I, Verhoeven E, Nusinow DA, Panning B, Marahrens Y, van Lohuizen M. Stable X chromosome inactivation involves the PRC1 Polycomb complex and requires histone MACROH2A1 and the CULLIN3/SPOP ubiquitin E3 ligase. Proc Natl Acad Sci U S A. 2005; 102:7635–7640. [PubMed: 15897469]

Hollander MC, Blumenthal GM, Dennis PA. PTEN loss in the continuum of common cancers, rare syndromes and mouse models. Nat Rev Cancer. 2011; 11:289–301. [PubMed: 21430697]

Hudes G, Carducci M, Tomczak P, Dutcher J, Figlin R, Kapoor A, Staroslawska E, Sosman J, McDermott D, Bodrogi I, et al. Temsirolimus, Interferon Alfa, or Both for Advanced Renal-Cell Carcinoma. New England Journal of Medicine. 2007; 356:2271–2281. [PubMed: 17538086]

Hung M-C, Link W. Protein localization in disease and therapy. Journal of Cell Science. 2011; 124:3381–3392. [PubMed: 22010196]

Jiang Y, Zhang W, Kondo K, Klco JM, St. Martin TB, Dufault MR, Madden SL, Kaelin WG, Nacht M. Gene Expression Profiling in a Renal Cell Carcinoma Cell Line: Dissecting VHL and Hypoxia-Dependent Pathways. Molecular Cancer Research. 2003; 1:453–462. [PubMed: 12692265]

Kaelin WG Jr. The von Hippel-Lindau tumour suppressor protein: O2 sensing and cancer. Nat Rev Cancer. 2008; 8:865–873. [PubMed: 18923434]

Kaelin WG Jr. Molecular basis of the VHL hereditary cancer syndrome. Nat Rev Cancer. 2002; 2:673–682. [PubMed: 12209156]

Kaelin WG Jr. The von Hippel-Lindau tumour suppressor protein: O2 sensing and cancer. Nat Rev Cancer. 2008; 8:865–873. [PubMed: 18923434]

Kapoor A, Figlin RA. Targeted inhibition of mammalian target of rapamycin for the treatment of advanced renal cell carcinoma. Cancer. 2009; 115:3618–3630. [PubMed: 19479976]

Kass EM, Ahn J, Tanaka T, Freed-Pastor WA, Keezer S, Prives C. Stability of Checkpoint Kinase 2 Is Regulated via Phosphorylation at Serine 456. Journal of Biological Chemistry. 2007; 282:30311–30321. [PubMed: 17715138]

Kent D, Bush EW, Hooper JE. Roadkill attenuates Hedgehog responses through degradation of Cubitus interruptus. Development. 2006; 133:2001–2010. [PubMed: 16651542]

Keyse SM. Dual-specificity MAP kinase phosphatases (MKPs) and cancer. Cancer Metastasis Rev. 2008; 27:253–261. [PubMed: 18330678]

Kim J, Kato M, Beachy PA. Gli2 trafficking links Hedgehog-dependent activation of Smoothened in the primary cilium to transcriptional activation in the nucleus. Proceedings of the National Academy of Sciences. 2009; 106:21666–21671.

Kim WY, Kaelin WG. Role of VHL gene mutation in human cancer. J Clin Oncol. 2004; 22:4991–5004. [PubMed: 15611513]

Kucejova B, Peña-Llopis S, Yamasaki T, Sivanand S, Tran TAT, Alexander S, Wolff NC, Lotan Y, Xie X-J, Kabbani W, et al. Interplay Between pVHL and mTORC1 Pathways in Clear-Cell Renal Cell Carcinoma. Molecular Cancer Research. 2011; 9:1255–1265. [PubMed: 21798997]

Kwon JE, La M, Oh KH, Oh YM, Kim GR, Seol JH, Baek SH, Chiba T, Tanaka K, Bang OS, et al. BTB domain-containing speckle-type POZ protein (SPOP) serves as an adaptor of Daxx for ubiquitination by Cul3-based ubiquitin ligase. J Biol Chem. 2006; 281:12664–12672. [PubMed: 16524876]

Lee HJ, Kim DI, Kang GH, Kwak C, Ku JH, Moon KC. Phosphorylation of ERK1/2 and prognosis of clear cell renal cell carcinoma. Urology. 2009; 73:394–399. [PubMed: 18849062]

Lee JO, Yang H, Georgescu MM, Di Cristofano A, Maehama T, Shi Y, Dixon JE, Pandolfi P, Pavletich NP. Crystal structure of the PTEN tumor suppressor: implications for its phosphoinositide phosphatase activity and membrane association. Cell. 1999; 99:323–334. [PubMed: 10555148]

Li C, Ao J, Fu J, Lee DF, Xu J, Lonard D, O'Malley BW. Tumor-suppressor role for the SPOP ubiquitin ligase in signal-dependent proteolysis of the oncogenic co-activator SRC-3/AIB1. Oncogene. 2011

Liu J, Ghanim M, Xue L, Brown CD, Iossifov I, Angeletti C, Hua S, Negre N, Ludwig M, Stricker T, et al. Analysis of Drosophila segmentation network identifies a JNK pathway factor overexpressed in kidney cancer. Science. 2009; 323:1218–1222. [PubMed: 19164706]

Lopez-Beltran A, Scarpelli M, Montironi R, Kirkali Z. 2004 WHO classification of the renal tumors of the adults. Eur Urol. 2006; 49:798–805. [PubMed: 16442207]

McDermott DF, Regan MM, Clark JI, Flaherty LE, Weiss GR, Logan TF, Kirkwood JM, Gordon MS, Sosman JA, Ernstoff MS, et al. Randomized phase III trial of high-dose interleukin-2 versus subcutaneous interleukin-2 and interferon in patients with metastatic renal cell carcinoma. J Clin Oncol. 2005; 23:133–141. [PubMed: 15625368]

Miyazaki K, Kawamoto T, Tanimoto K, Nishiyama M, Honda H, Kato Y. Identification of Functional Hypoxia Response Elements in the Promoter Region of the DEC1 and DEC2 Genes. Journal of Biological Chemistry. 2002; 277:47014–47021. [PubMed: 12354771]

Motzer RJ, Escudier B, Tomczak P, Hutson TE, Michaelson MD, Negrier S, Oudard S, Gore ME, Tarazi J, Hariharan S, et al. Axitinib versus sorafenib as second-line treatment for advanced renal

cell carcinoma: overall survival analysis and updated results from a randomised phase 3 trial. The Lancet Oncology. 2013; 14:552–562. [PubMed: 23598172]

Motzer RJ, Hutson TE, Tomczak P, Michaelson MD, Bukowski RM, Rixe O, Oudard S, Negrier S, Szczylik C, Kim ST, et al. Sunitinib versus interferon alfa in metastatic renal-cell carcinoma. N Engl J Med. 2007; 356:115–124. [PubMed: 17215529]

Motzer RJ, Molina AM. Targeting renal cell carcinoma. J Clin Oncol. 2009; 27:3274–3276. [PubMed: 19451422]

Myers MP, Pass I, Batty IH, Van der Kaay J, Stolarov JP, Hemmings BA, Wigler MH, Downes CP, Tonks NK. The lipid phosphatase activity of PTEN is critical for its tumor supressor function. Proceedings of the National Academy of Sciences of the United States of America. 1998; 95:13513–13518. [PubMed: 9811831]

Nagai Y, Kojima T, Muro Y, Hachiya T, Nishizawa Y, Wakabayashi T, Hagiwara M. Identification of a novel nuclear speckle-type protein, SPOP. FEBS Lett. 1997; 418:23–26. [PubMed: 9414087]

Nardozzi JD, Lott K, Cingolani G. Phosphorylation meets nuclear import: a review. Cell Commun Signal. 2010; 8:32. [PubMed: 21182795]

Negrier S, Escudier B, Lasset C, Douillard JY, Savary J, Chevreau C, Ravaud A, Mercatello A, Peny J, Mousseau M, et al. Recombinant human interleukin-2, recombinant human interferon alfa-2a, or both in metastatic renal-cell carcinoma. Groupe Francais d'Immunotherapie. N Engl J Med. 1998; 338:1272–1278. [PubMed: 9562581]

Network, T. C. G. A. R. Comprehensive molecular characterization of clear cell renal cell carcinoma. Nature. 2013; 499:43–49. [PubMed: 23792563]

Nickerson ML, Jaeger E, Shi Y, Durocher JA, Mahurkar S, Zaridze D, Matveev V, Janout V, Kollarova H, Bencko V, et al. Improved identification of von Hippel-Lindau gene alterations in clear cell renal tumors. Clin Cancer Res. 2008; 14:4726–4734. [PubMed: 18676741]

Patterson KI, Brummer T, O'Brien PM, Daly RJ. Dual-specificity phosphatases: critical regulators with diverse cellular targets. Biochem J. 2009; 418:475–489. [PubMed: 19228121]

Polo JM, Ci W, Licht JD, Melnick A. Reversible disruption of BCL6 repression complexes by CD40 signaling in normal and malignant B cells. Blood. 2008; 112:644–651. [PubMed: 18487509]

Rini BI, Campbell SC, Escudier B. Renal cell carcinoma. Lancet. 2009; 373:1119–1132. [PubMed: 19269025]

Robb VA, Karbowniczek M, Klein-Szanto AJ, Henske EP. Activation of the mTOR signaling pathway in renal clear cell carcinoma. J Urol. 2007; 177:346–352. [PubMed: 17162089]

Salomoni P, Khelifi AF. Daxx: death or survival protein? Trends Cell Biol. 2006; 16:97–104. [PubMed: 16406523]

Sansal I, Sellers WR. The biology and clinical relevance of the PTEN tumor suppressor pathway. J Clin Oncol. 2004; 22:2954–2963. [PubMed: 15254063]

Sarbassov DD, Ali SM, Sabatini DM. Growing roles for the mTOR pathway. Current Opinion in Cell Biology. 2005; 17:596–603. [PubMed: 16226444]

Sasaki H, Nishizaki Y, Hui C, Nakafuku M, Kondoh H. Regulation of Gli2 and Gli3 activities by an amino-terminal repression domain: implication of Gli2 and Gli3 as primary mediators of Shh signaling. Development. 1999; 126:3915–3924. [PubMed: 10433919]

Sato Y, Yoshizato T, Shiraishi Y, Maekawa S, Okuno Y, Kamura T, Shimamura T, Sato-Otsubo A, Nagae G, Suzuki H, et al. Integrated molecular analysis of clear-cell renal cell carcinoma. Nat Genet. 2013; 45:860–867. [PubMed: 23797736]

Shinojima T, Oya M, Takayanagi A, Mizuno R, Shimizu N, Murai M. Renal cancer cells lacking hypoxia inducible factor (HIF)-1alpha expression maintain vascular endothelial growth factor expression through HIF-2alpha. Carcinogenesis. 2007; 28:529–536. [PubMed: 16920734]

The Cancer Genome Atlas Research, N. Comprehensive molecular characterization of clear cell renal cell carcinoma. Nature. 2013; 499:43–49. [PubMed: 23792563]

Vivanco I, Sawyers CL. The phosphatidylinositol 3-Kinase-AKT pathway in human cancer. Nat Rev Cancer. 2002; 2:489–501. [PubMed: 12094235]

Wang C, Pan Y, Wang B. Suppressor of fused and Spop regulate the stability, processing and function of Gli2 and Gli3 full-length activators but not their repressors. Development. 137:2001–2009. [PubMed: 20463034]

Wardle EN. Cyclophosphamide pulse therapy in relapsing nephrotic syndrome. Nephron. 1991; 58:377. [PubMed: 1896110]

Wu X, Senechal K, Neshat MS, Whang YE, Sawyers CL. The PTEN/MMAC1 tumor suppressor phosphatase functions as a negative regulator of the phosphoinositide 3-kinase/Akt pathway. Proc Natl Acad Sci U S A. 1998; 95:15587–15591. [PubMed: 9861013]

Xu L, Wei Y, Reboul J, Vaglio P, Shin TH, Vidal M, Elledge SJ, Harper JW. BTB proteins are substrate-specific adaptors in an SCF-like modular ubiquitin ligase containing CUL-3. Nature. 2003; 425:316–321. [PubMed: 13679922]

Zhang Q, Zhang L, Wang B, Ou CY, Chien CT, Jiang J. A hedgehog-induced BTB protein modulates hedgehog signaling by degrading Ci/Gli transcription factor. Dev Cell. 2006; 10:719–729. [PubMed: 16740475]

Zhuang M, Calabrese MF, Liu J, Waddell MB, Nourse A, Hammel M, Miller DJ, Walden H, Duda DM, Seyedin SN, et al. Structures of SPOP-substrate complexes: insights into molecular architectures of BTB-Cul3 ubiquitin ligases. Mol Cell. 2009; 36:39–50. [PubMed: 19818708]

Highlights

- Transcriptional factor HIF can regulate the expression of SPOP in ccRCC
- Hypoxia drives SPOP accumulation in ccRCC cell cytoplasm which promotes tumorigenesis
- SPOP mediates the ubiquitination and degradation of PTEN and DUSP7
- SPOP targets, PTEN, DUSP7, DAXX and Gli2, are downregulated in all primary ccRCC

Significance

Tumor cells can adapt to hypoxic microenvironments in several different ways to promote tumor growth including stimulating angiogenesis. Herein, we demonstrate that hypoxia can drive the cytoplasmic accumulation of SPOP, and that cytoplasmic accumulation of SPOP is sufficient to convey tumorigenic properties onto otherwise non-tumorigenic cells by targeting PTEN and several other tumor suppressor molecules for E3 ligase mediated degradation. This tumor-promoting function of SPOP stands in contrast to its pro-apoptotic role in the cell nucleus. These results have elucidated a major mechanism that contributes to tumorigenesis in ccRCC, connecting hypoxia response and ubiquitin-mediated degradation of tumor suppressors. The oncogenic role of cytoplasmic SPOP makes it a promising candidate for therapeutic intervention.

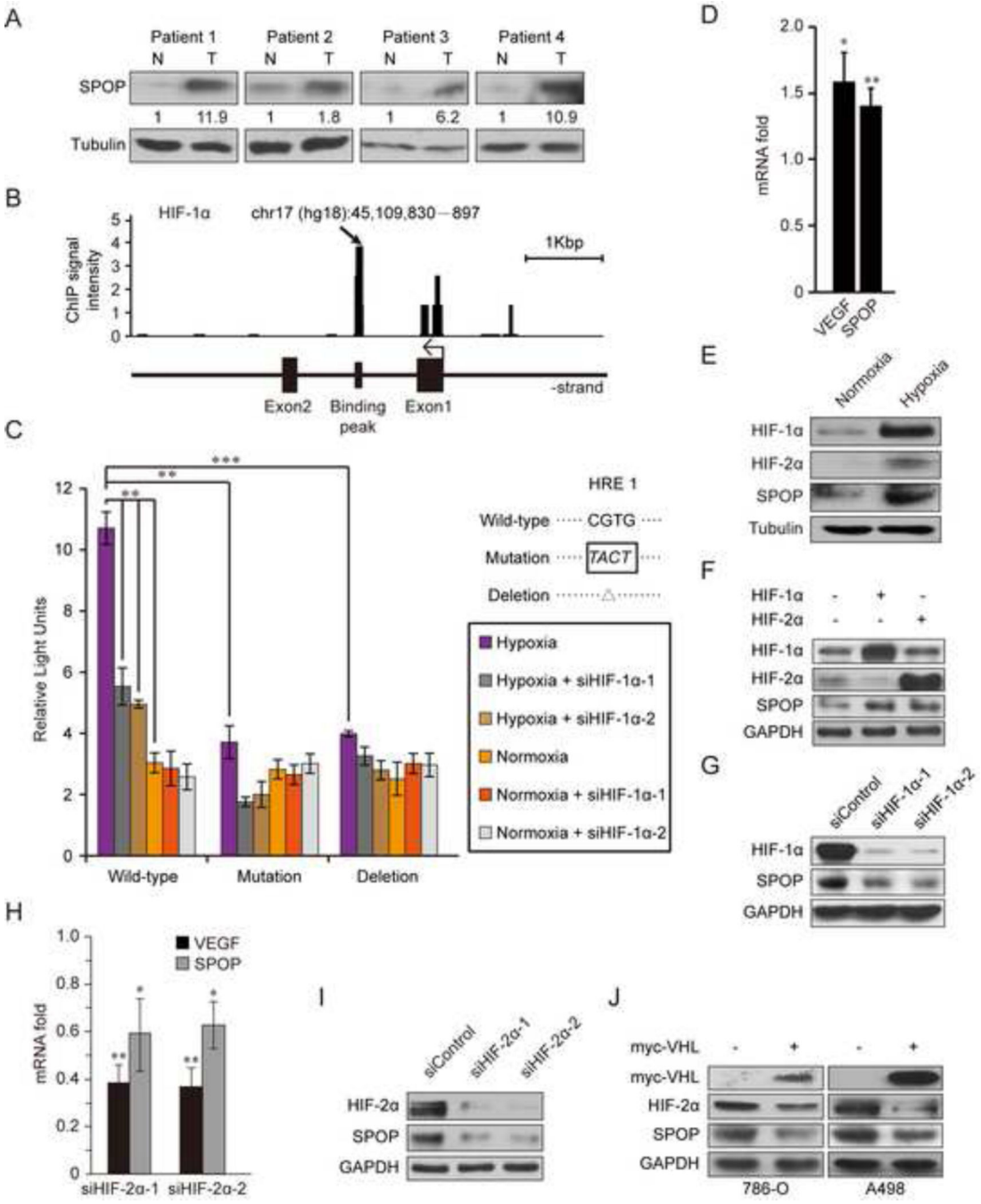

Figure 1. HIF activates SPOP expression

(A) Immunoblots of endogenous SPOP in four paired ccRCC tumor and adjacent non-tumor tissue samples. Numbers indicate the relative density of the tumor tissue verse normal tissue as evaluated using Image J software. SPOP was detected by immunoblotting with an anti-SPOP antibody (clone 6C). Tubulin was used as a loading control.

(B) HIF-1α ChIP-seq peak within the first intron of the SPOP gene (arrow). ChIP signal intensity represents differential binding between input/mock IP control and HIF-1α antibody ChIP. The ChIP signal intensity represents the differential binding.

(C) Luciferase reporter assays indicate that the HIF binding peak in the first intron of SPOP (chr17: 45,032,738–890) is functional. The wild-type and HRE (CGTG) mutated or deleted HIF binding sequence were cloned into a pGL3-promoter vector. Luciferase activities were normalized to Renella luciferase, and the results are represented as values relative to the empty vector. Hypoxia was induced using a hypoxia chamber (1% O_2/5% CO_2/94% N_2). RNAi knockdown was performed with two independent siRNAs to HIF-1α.

(D) SPOP mRNA expression is activated under hypoxic conditions in the Caki-2 ccRCC cell line. VEGF was used as a positive control.

(E) SPOP protein abundance increases after hypoxia treatment in Caki-2 cells. Tubulin was used as a loading control.

(F) In either HIF-1α- or HIF-2α-transfected HEK293 cells, SPOP protein expression was induced. GAPDH was used as a loading control.

(G) Knockdown HIF-1α down-regulated the expression of SPOP in Caki-2 cells. RNAi knockdown was performed as Figure 1C.

(H) SPOP mRNA expression is suppressed after two independent siRNAs knockdown of HIF-2α in 786-O ccRCC cells. mRNA expression was normalized to control cells exposed to negative control siRNAs. VEGF was used as a positive control.

(I) SPOP protein abundance decreases after knockdown of HIF-2α in A498 cells. Tubulin was used as a loading control.

(J) SPOP protein abundance decreases when restoring of VHL in 786-O and A498 cells. Cells were harvested 72 hr after transfection. GAPDH was used as a loading control.

Data in (C), (D), and (H) are presented as mean ± SD of at least three independent experiments. *$p < 0.05$, **$p < 0.01$ and ***$p < 0.001$ based on Student's t test. See also Figure S1.

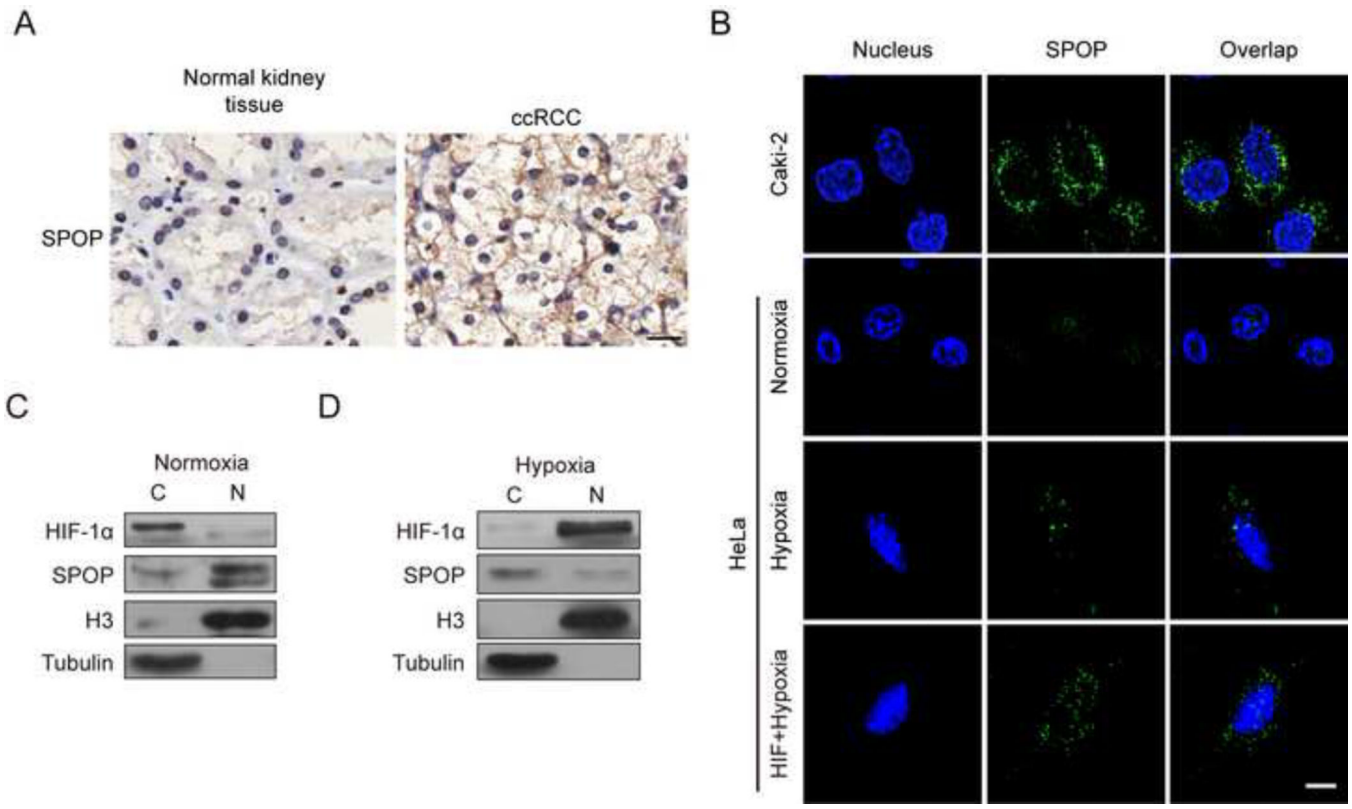

Figure 2. Hypoxia drives SPOP accumulation in the cytoplasm of ccRCC cells

(A) Immunohistochemistry reveals that SPOP accumulates in the cytoplasm of ccRCC tumor cells but in the nuclei of adjacent non-tumor cells. An SPOP-specific monoclonal antibody (SPOP-5G) was used for staining (diaminobenzidine, brown staining). Scale bar, 20μm.

(B) SPOP localizes in the nucleus in HeLa cells under normoxic conditions but accumulates in the cytoplasm under hypoxic conditions (1% O_2), comparable to that in Caki-2 cells; additional HIF expression enhances SPOP accumulation in the cytoplasm. Cells were stained with SPOP-5G antibody (green), and the nuclei were counterstained with DAPI (4', 6-diamidino-2-phenylindole, blue). Scale bar, 10μm.

(C) Separation of the nuclear (N) and cytoplasmic (C) fractions confirms SPOP accumulation in the cytoplasm of HeLa cells under mormoxic conditions. Histone H3 and tubulin served as nuclear and cytoplasmic markers, respectively.

(D) Separation of the nuclear (N) and cytoplasmic (C) fractions confirms SPOP accumulation in the cytoplasm of HeLa cells under hypoxic conditions (1% O_2). Histone H3 and tubulin served as nuclear and cytoplasmic markers, respectively.

See also Figure S2.

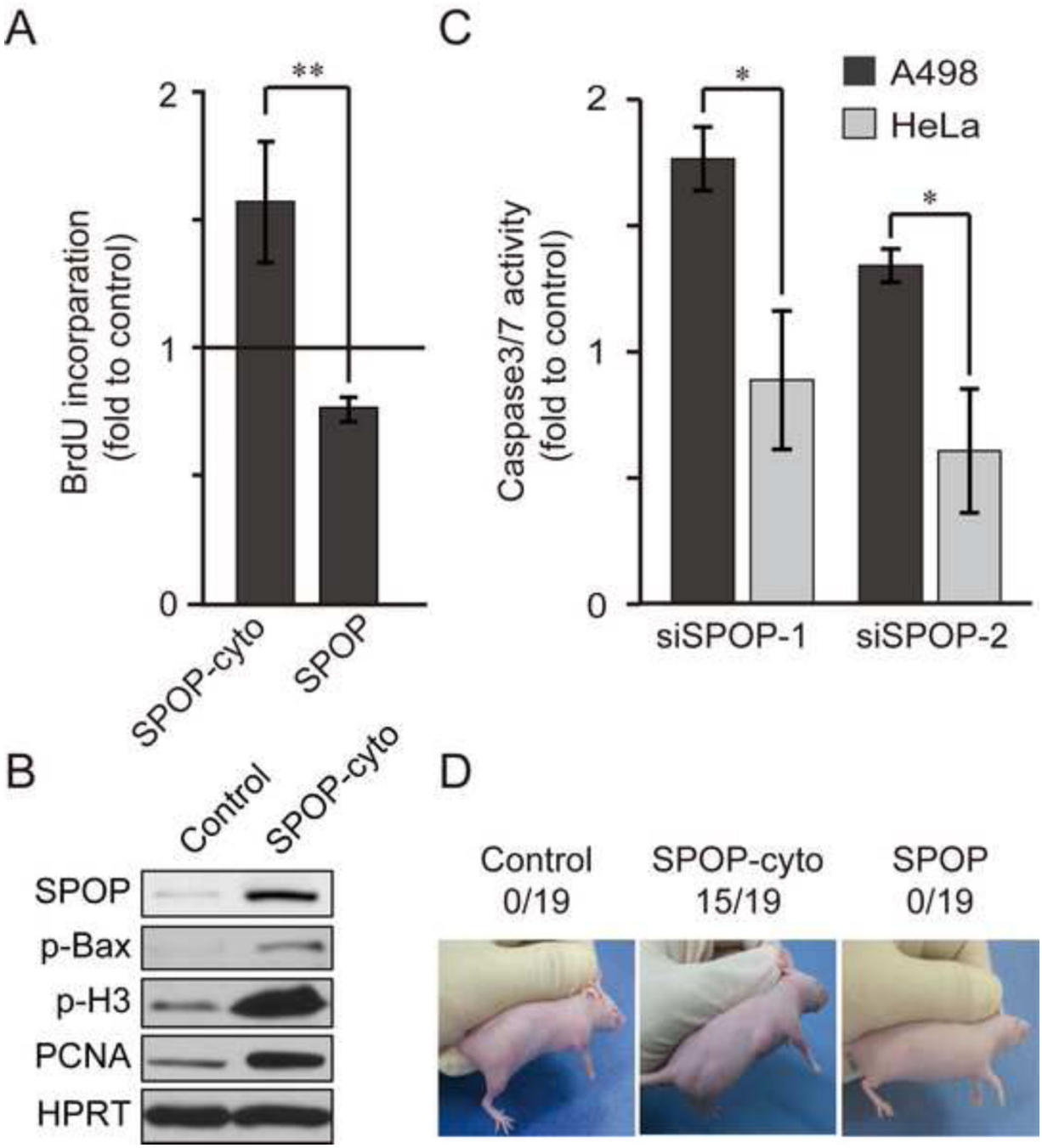

Figure 3. Cytoplasmic SPOP promotes tumorigenesis

(A) SPOP-cyto promotes cell proliferation. HEK293 cells were transfected with the indicated vectors for 48 hr, and cell proliferation was measured by BrdU incorporation. Values are normalized to empty vector-transfected control cells.

(B)SPOP-cyto overexpression upregulates the indicated anti-apoptotic marker ser184-phosphorylated Bax (p-Bax) and proliferation markers, ser10-phosphorylated histone H3 (p-Histone H3) and Proliferating Cell Nuclear Antigen (PCNA). SPOP-5G antibody was used to blot SPOP. HPRT served as a loading control.

(C) RNAi knockdown of SPOP induces apoptosis in A498 but not HeLa cells. Apoptosis was evaluated by caspase 3/7 activity 48 h after siRNA transfection.
(D) SPOP-cyto promotes tumorigenesis in a xenograft model. HEK293-pcDNA3, HEK293-SPOP or HEK293-SPOP-cyto polyclonal stable cell lines were injected subcutaneously into the nude mice. Six weeks later, the number of mice that formed tumors in each group was counted.
Data in (A) and (C) are presented as the mean ± SD of three independent experiments. *$p < 0.05$ and **$p < 0.01$ based on Student's t test. See also Figure S3.

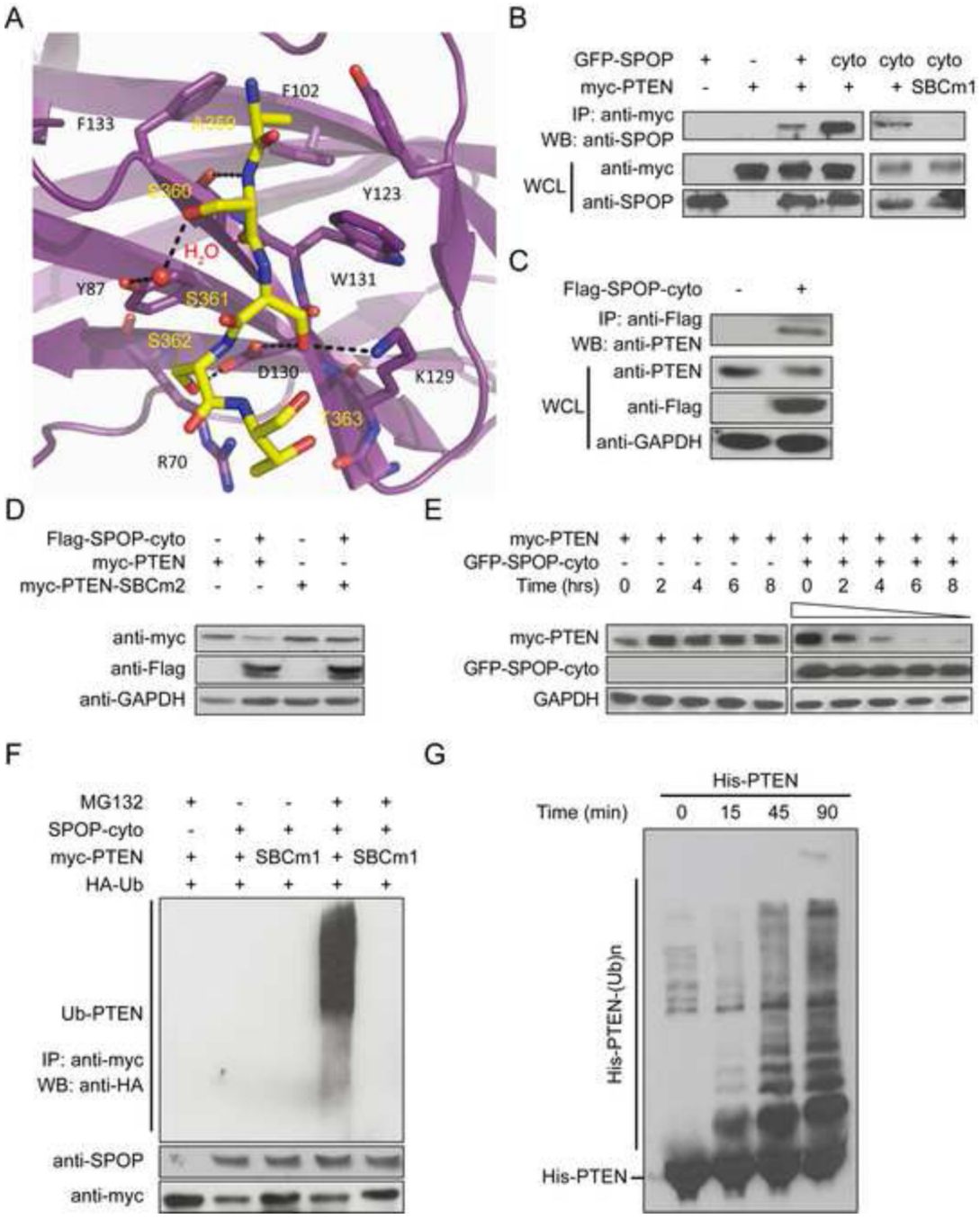

Figure 4. SPOP mediates the ubiquitination and degradation of PTEN

(A) Crystal structure of the SPOP MATH domain complex with a peptide corresponding to the PTEN SBC motif.

(B) Co-immunoprecipitation reveals that SPOP and SPOP-cyto bind PTEN, whereas a PTEN mutant lacking a functional SBC motif (SBC1, deletion of the SBC peptide residues 359–363) is unable to bind SPOP. HeLa cells were transfected with the indicated plasmids and incubated with 10 μM MG132 for 4 hours before harvesting. GFP-SPOP and GFP-

SPOP-cyto were detected with monoclonal antibody SPOP-6C.WCL represents whole cell lysates.

(C) Co-immunoprecipitation and immunoblots indicate that overexpressed SPOP-cyto can interact with and degrade endogenous PTEN in HeLa cells. GAPDH served as a loading control. WCL represents whole cell lysates.

(D) SPOP promotes the degradation of PTEN but not a PTEN SBC mutant (SBC2: the SBC motif ASSST was replaced with GGSGG). GAPDH was used as a loading control.

(E) Measurement of PTEN protein abundance by cycloheximide (CHX) chase assay. HEK293 cells were transfected with the indicated plasmids. Thirty-six hours after transfection, the cells were treated with CHX (100 μg/ml) for 2–8 h, and western blotting was performed. GFP-SPOP-cyto was detected with monoclonal antibody SPOP-6C. GAPDH was used as a loading control.

(F) Knockdown of SPOP by siRNA induces PTEN protein accumulation and increased phospho-Akt (Thr308) levels in A498 cells. SPOP was detected with monoclonal antibody SPOP-6C.

(F) *In vivo* ubiquitination assay reveals that SPOP promotes PTEN ubiquitination through the PTEN SBC domain. Cell lysates were prepared under denaturing conditions. Myc-PTEN was immunoprecipitated and HA-Ub was detected by immunoblot.

(G) *In vitro* ubiquitination assay demonstrates that PTEN is a substrate of SPOP. See also Table S1 and Figure S4.

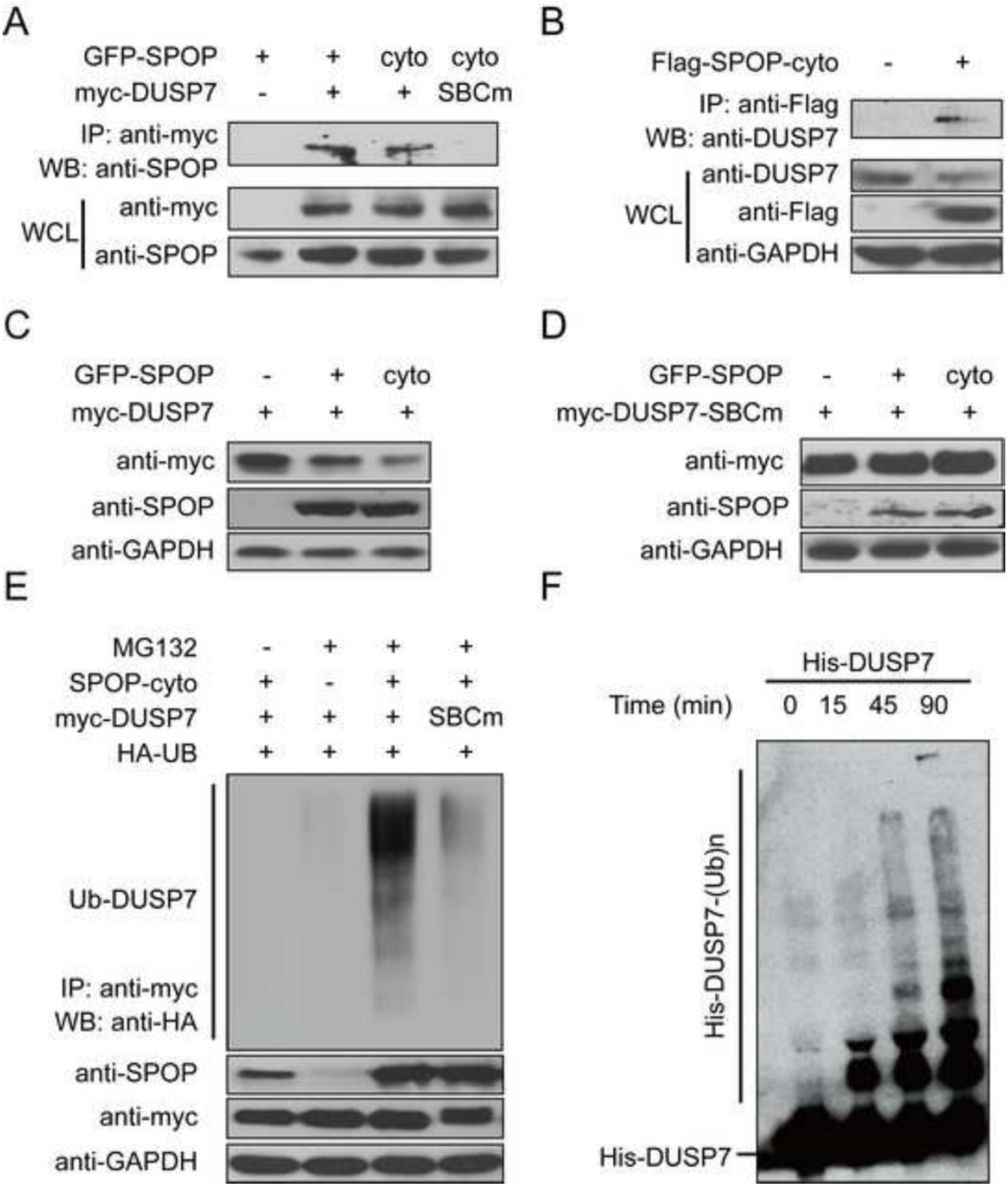

Figure 5. SPOP mediates the ubiquitination and degradation of DUSP7

(A) Ectopically expressed SPOP or SPOP-cyto can interact with DUSP7 in an *in vivo* co-immunoprecipitation (co-IP) assay, whereas DUSP7-SBCm (replace SBC motif VDSSS with VDGGG) eliminates the interaction. HeLa cells were transfected with the indicated constructs and incubated with 10 μM MG132 for 4 hours before harvesting.

(B) Co-immunoprecipitation and immunoblots indicate that overexpressed SPOP-cyto can interact and degrade endogenous DUSP7 in HeLa cells. GAPDH served as a loading control.

(C) SPOP promotes DUSP7 degradation. HEK293 cells were transfected with the indicated constructs. GFP-SPOP and GFP-SPOP-cyto were detected with monoclonal antibody SPOP-6C. GAPDH was used as loading control.
(D) Immunoblots demonstrate that neither SPOP nor SPOP-cyto can degrade DUSP7-SBCm.
(E) *In vivo* ubiquitination assay reveals that SPOP promotes DUSP7 ubiquitination through the DUSP7 SBC domain. Cell lysates were prepared under denaturing condition. Myc-DUSP7 was immunoprecipitated, and HA-Ub was detected by immunoblotting.
(F) *In vitro* ubiquitination assay demonstrates that DUSP7 is a substrate of SPOP.
See also Figure S5.

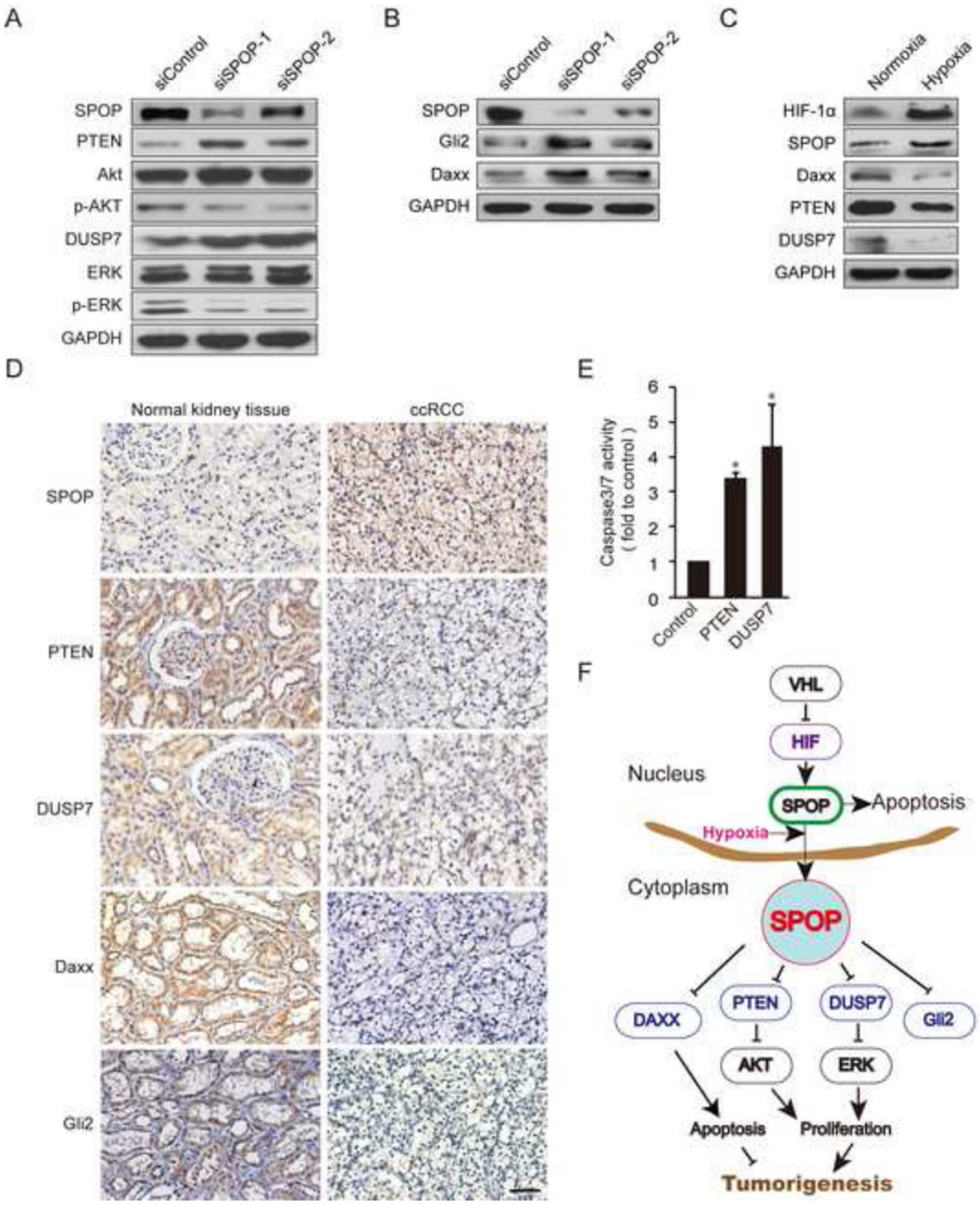

Figure 6. SPOP regulates multiple targets in kidney cancer

(A) Immunoblots indicate that knockdown of SPOP induces PTEN and DUSP7 protein accumulation and decreased phosphor-Akt (Thr308) and phospho-ERK (Thr202/Tyr204) levels in A498 cells. GAPDH served as a loading control.

(B) Immunoblots demonstrate that knockdown of SPOP in Caki-2 cells induced Daxx and Gli2 protein accumulation. GAPDH was used as loading control.

(C) Daxx, PTEN and DUSP7 protein abundance decrease under hypoxia treatment in HeLa cells.

(D) Immunohistochemistry staining indicates a reduction in multiple SPOP targets, PTEN, DUSP7, Daxx and, in ccRCCs patient samples compared with their adjacent normal tissues (diaminobenzidine, brown staining). One pair of representative samples is shown. Scale bar, 50μm.

(E) Restoring of PTEN and DUSP7 induces apoptosis in A498. Caspase 3/7 activity was analyzed to evaluate cell apoptosis. Values were normalized to control and expressed as mean ± SD of three independent experiments. *$p < 0.05$ based on Student's t test.

(F) Schematic overview of SPOP action as a regulatory hub in promoting tumorigenesis in ccRCC. Although SPOP is localized to the nucleus in normal cells, in cancer cells it accumulates in the cytoplasm and promotes tumorigenesis by targeting tumor suppressor (PTEN, DUSP7, Gli2) and pro-apototic protein (Daxx) for ubiquitin-mediated degradation. See also Figure S6.